Hydrogen bonded liquid crystals from nitrophenols and alkoxystilbazoles

Daniel J. Price,[‡b] Kimberley Willis,[b] Tim Richardson,[b] Goran Ungar[b] and Duncan W. Bruce*[a]

[a]*Department of Chemistry, University of Exeter, Stocker Road, Exeter, UK EX4 4QD*
Fax: +44 1392 263434. Email: d.bruce@exeter.ac.uk.
[b]*Centre for Molecular Materials, Dainton Building, University of Sheffield, Sheffield, UK S3 7HF*

Three series of hydrogen bonded adducts have been formed between 4-alkoxy-4′-stilbazoles[†] and the nitrophenols 4-nitrophenol, 3-nitrophenol and 2,4-dinitrophenol. Each series is mesomorphic displaying both nematic and smectic A phases, in sharp contrast to the behaviour of the individual components. The binary phase behaviour of mixtures of 3-nitrophenol and 4-octyloxystilbazole is reported, and gives conclusive evidence for the formation of a one-to-one hydrogen bonded adduct. Electronic spectroscopy of 2,4-dinitrophenol/decyloxystilbazole was very informative and showed that the higher energy, ionic hydrogen bonded state, corresponding to proton transfer, was significantly populated through the mesophase, and that the mesophase provides an additional stabilisation for this state.

Introduction

In the field of liquid crystals, hydrogen bonding has long been recognised as crucial to mesophase formation in certain systems. An early, and now classic, example is that of the alkoxybenzoic acids,[1] where dimerisation of the molecules gives enhanced structural anisotropy. Another class of hydrogen bonded mesogen are the alkylsilanediols,[2] the aggregation of which has been the subject of investigation.[3] The silanediols are in turn related to the large class of mesomorphic polyalcohols, characterised by periodicity within the mesophase structure, and including compounds from the straight chain α,β,ψ-alkanetetraols,[4] to carbohydrates.[5] In the latter case, mesophase formation is driven by a microphase separation of different parts (polar and non-polar) of the molecules.

More recently, the results of studies of complementary heteromeric hydrogen bonded systems have been reported.[6] Lehn and co-workers[7] demonstrated induced mesomorphism in 'pseudo' main-chain polymers and low molecular mass materials self-assembled from complex, complementary parts. On a similar theme but at a structurally simpler level Yu,[8] Griffin,[9] ourselves[10] and particularly Kato,[11] and their respective co-workers, have described many mesomorphic materials based on the adducts formed between substituted pyridines and carboxylic acid groups.

Alongside work based on this carboxylic acid pyridyl interaction, we have examined liquid crystalline systems where the proton donor is a phenol. We demonstrated monotropic mesomorphism in complexes of 4-cyanophenol with 4-alkoxystilbazoles,[12] and, more recently, enantiotropic nematic and smectic A phases in complexes of 3-cyanophenol with 4-alkoxystilbazoles,[13] showing how structural anisotropy, and hence mesophase stability, can be simply controlled in these complexes. It was also clear that the phenol–stilbazole hydrogen bond was sufficiently strong to allow the formation of mesophases from the complexes.

Having studied these cyanophenols, we then turned our attention to nitrophenols as other examples of phenols bearing polarisable groups, and three series of complexes containing nitrophenols were prepared.

Mesomorphism of the Complexes

Hydrogen bonded adducts were formed between 4-alkoxystilbazole and the following nitrophenols: 4-nitrophenol, 3-nitrophenol and 2,4-dinitrophenol. Each of these complexes will be referred to by the abbreviated format **X-N*n***; where **X** refers to the position of substitution on the phenol and ***n*** is the length of the carbon chain on the stilbazole (thus, **2,4-N6** would represent the complex between hexyloxystilbazole and 2,4-dinitrophenol).

The proposed structures of these complexes are shown below; variation of the alkyl chain length, *n*, of the stilbazole gave three homologous series. The mesomorphism of these materials was studied by optical microscopy and differential scanning calorimetry (DSC). The phase behaviour, transition temperatures and associated thermal parameters are given in Tables 1–3.

The behaviour of these adducts is very different to that shown by the individual components. For example, the alkoxystilbazoles[14] show a narrow range of smectic B and crystal smectic E phases, typically between 80 and 90 °C, while the 4-nitro-, 3-nitro- and 2,4-dinitro-phenols simply melt at 113, 96 and 108 °C, respectively.

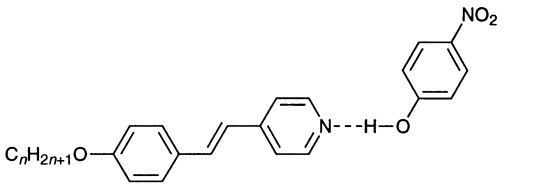

4-N*n*

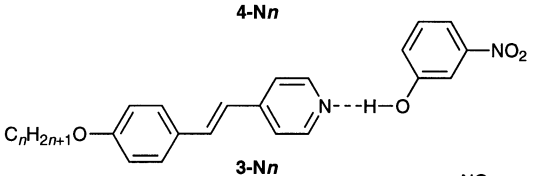

3-N*n*

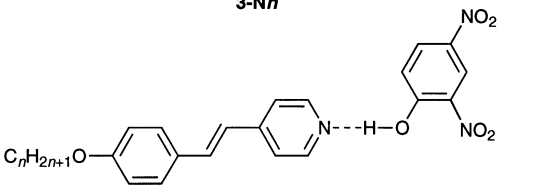

2,4-N*n*

Complexes of 4-nitrophenol with 4-alkoxystilbazole (4-N*n*)

This series has the phase behaviour shown in Fig. 1. Monotropic nematic phases are seen for homologues from methoxy (**4-N**1) to octyloxy (**4-N**8). The nonyloxy derivative (**4-N**9) sees the onset of smectic behaviour, with both nonyloxy (**4-N**9) and decyloxy (**4-N**10) derivatives showing monotropic

† Stilbazole = styrylpyridine; 4′-stilbazole denotes attachment at the 4-position of the pyridine ring.
‡ *Current address*: School of Chemical Sciences, University of East Anglia, University Plain, Norwich, UK NR4 7TJ.

Table 1 Mesomorphism, and associated enthalpies and entropies for the **4-N*n*** series of hydrogen bonded adducts; monotropic transitions are indicated by parentheses

complex	transition	t/°C	ΔH /kJ mol^{-1}	ΔS /J K^{-1} mol^{-1}
4-N1	Crys–I	118	35.2	91
	(N–I)	88	—[a]	
4-N2	Crys–I	101	31.8	85
	(N–I)	85	0.68	1.9
4-N3	Crys–I	100	32.2	98
	(N–I)	(70)	(0.4)	(1.2)
4-N4	Crys–I	93	27.6	75.5
	(N–I)	(79)	(0.4)	(1.1)
4-N5	Crys–I	82	36.6	103
	(N–I)	(71)	(0.41)	(1.2)
4-N6	Crys–I	97	42.2	115
	(N–I)	(77)	(0.4)	(1.0)
4-N7	Crys–I	92	47.8	131
	(N–I)	(77)	(0.42)	(1.2)
4-N8	Crys–I	99	51.7	139
	(N–I)	(80)	(0.85)	(2.4)
4-N9	Crys–I	93	52.3	143
	(Crys′–N)	(79)	(41.9)	(122)
	(S_A–N)	(70)	[b]	
	(N–I)	(82)	(1.07)	(3.0)
4-N10	Crys–I	97	57.4	155
	(S_A–N)	(84)	[b]	
	(N–I)	(86)	(−0.83)[c]	(−2.3)
4-N11	Crys–I	90	56.3	155
	(Crys′–S_A)	(80)	—[a]	
	S_A–I	89	2.50	6.9
4-N12	Crys–S_A	80	36.4	103
	(Crys′–S_A)	(74)	—[a]	
	S_A–I	91	2.98	8.2
4-N13	Crys–S_A	88	54.9	152
	S_A–I	95	3.50	9.5

[a]Denotes a transition not seen in the DSC experiment. [b]Indicates a second order transition. [c]Indicates where monotropic transitions could not be seen or resolved as part of a heating cycle, and therefore the cooling cycle was used.

Table 2 Mesomorphism, and associated enthalpies and entropies for the **3-N*n*** series; monotropic transitions are indicated by parentheses

complex	transition	t/°C	ΔH /kJ mol^{-1}	ΔS /J K^{-1} mol^{-1}
3-N1	Crys–I	98	33.0	89
	(N–I)	(97)	(1.01)	(2.7)
3-N2	Crys–I	114	37.2	96
	(N–I)	(99)	—[a]	
3-N3	Crys–I	90	33.2	92
	(N–I)	(83)	(0.82)	(2.3)
3-N4	Crys–N	66	35.5	105
	(Crys′–N)	(60)	(24.8)	(75.0)
	N–I	89	0.93	2.6
3-N5	Crys–N	60	28.5	86
	N–I	84	0.54	1.5
3-N6	Crys–N	79	44.6	126
	N–I	88	0.7	1.8
3-N7	Crys–N	81	41.5	118
	N–I	86	0.55	1.5
3-N8	Crys–N	75	41.9	120
	(Crys′–N)	(74)	—[a]	
	N–I	90	0.84	2.3
3-N9	Crys–N	71	44.2	129
	(Crys′–N)	(70)	—[a]	
	N–I	86	0.77	2.2
3-N10	Crys–S_A	78	51.8[b]	148[b]
	S_A–N	79		
	N–I	90	1.11	3.1
3-N11	Crys–S_A	77	54.1	155
	S_A–N	87	0.22	0.61
	N–I	90	1.25	3.4
3-N12	Crys–S_A	80	56.5	160
	(Crys′–S_A)	(66)	—[a]	
	S_A–I	92	2.92	8.0
3-N13	Crys–S_A	79	64.6	184
	(Crys′–S_A)	(70)	—[a]	
	S_A–I	93	4.04	11

[a]Denotes a transition not seen in the DSC experiment. [b]Indicates combined enthalpies of transition where a baseline resolution was not obtained.

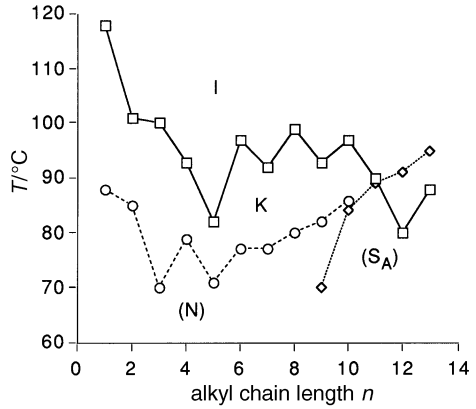

Fig. 1 The phase behaviour of the **4-N*n*** series: (□) K–, (◇) S_A–, (○) N–I

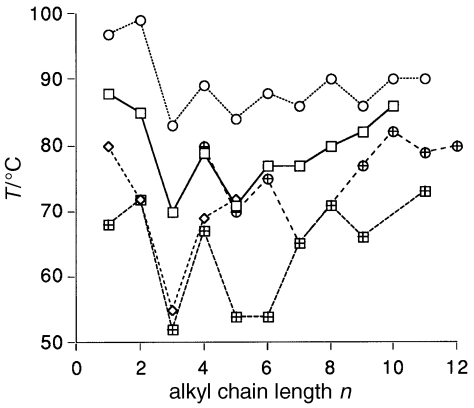

Fig. 2 Plot of nematic–isotropic transition temperature *vs.* chain length for complexes of stilbazoles with nitro- and cyano-phenols: (□) **4-N*n***, (○) **3-N*n***, (◇) **2,4-N*n***, (⊞) **4-C*n***, (⊕) **3-C*n***

smectic A and nematic phases. The **4-N**11 has just a monotropic smectic A phase, while for the **4-N**12 and **4-N**13 homologues, the combination of the continued destabilisation of the crystal phase and the increased stability of the smectic A phase resulted in enantiotropic behaviour.

This series of adducts can be compared with the analogous complexes formed between 4-cyanophenol and alkoxystilbazoles,[13] (**4-C*n***—this abbreviation refers to the analogous complexes with 4-cyanophenol). First, in the **4-N*n*** series the mesophases are more thermally stable (Fig. 2) by some 10–20 °C, which we tentatively attribute to enhanced antiparallel correlations induced by the nitro group in these systems. In both series, the smectic A phase is seen to replace the nematic phase at longer chain lengths, and in the nitro derivatives, this is a gradual change, with intermediate chain lengths showing both nematic and smectic A phases. In contrast, there is a sudden switch from nematic to smectic A in the analogous cyano derivatives. Thus, extensive supercooling of the nematic phase of **4-C**9 never revealed a smectic phase, yet **4-C**10 showed only a smectic A structure.

There are also similarities in the melting behaviour of both series. After initially decreasing from the high melting methoxy and ethoxy derivatives, an odd–even effect is seen in both cases, although this is more pronounced in the **4-N*n*** complexes. In both **4-N*n*** and **4-C*n*** complexes, we also noted the existence

Table 3 Mesomorphism, and associated enthalpies and entropies for the **2,4-N*n*** series; monotropic transitions are indicated by parentheses

complex	transition	t/°C	ΔH /kJ mol^{-1}	ΔS /J K^{-1} mol^{-1}
2,4-N1	Crys–I	150	43.2	102
	(Crys′–I)	(148)	—[a]	
	(N–I)	(80)	—[a]	
2,4-N2	Crys–I	157	44.8	104
	(Crys′–I)	(120)	—[a]	
	(N–I)	(72)	—[a]	
2,4-N3	Crys–I	139	47.8	117
	(Crys′–I)	(121)	—[a]	
	(N–I)	(55)	—[a]	
2,4-N4	Crys–I	114	41.9	103
	(Crys′–I)	(100)	—[a]	
	(N–I)	(69)	—[a]	
2,4-N5	Crys–I	114	49.3	127
	(Crys′–I)	(111)	—[a]	
	(N–I)	(72)	—[a]	
2,4-N6	Crys–I	113	42.8	112
	(S_A–I)	(85)	—[a]	
2,4-N7	Crys–I	101	36.5	99
	(Crys′–I)	(95)	—[a]	
	(S_A–I)	(94)	(2.53)	(7.0)
2,4-N8	Crys–S_A	95	37.4	103
	S_A–I	104	3.33	8.9
2,4-N9	Crys–S_A	98	48.2	130
	S_A–I	111	4.06	10.6
2,4-N10	Crys–S_A	97	44.7	121
	S_A–I	117	4.50	11.5
2,4-N11	Crys–S_A	101	59.2	159
	S_A–I	121	4.94	12.5
2,4-N12	Crys–S_A	97	47.2	129
	S_A–I	125	5.32	13.4
2,4-N13	Crys–S_A	97	45.2	122
	S_A–I	126	4.63	11.6

[a]Denotes a transition not seen in the DSC experiment.

of a second, metastable crystal polymorph which typically melted at some 10–20 °C lower than the more stable state. Finally, it was curious to note that the stability of the nematic phase of these complexes is higher than that of the related 3-cyanophenol complexes, despite the more advantageous structural anisotropy in the latter series.

Complexes of 3-nitrophenol with 4-alkoxystilbazole (3-N*n*)

The phase behaviour of this series of complexes is shown in Fig. 3. All derivatives with the exception of **3-N**1, **3-N**2 and **3-N**3 display enantiotropic mesomorphism. This series shows the largest thermal range of liquid crystal phases yet seen in complexes based on the phenol–pyridyl interaction. The nematic phase is seen for all homologues up to the **3-N**9, after which both the **3-N**10 and **3-N**11 derivatives are polymorphic showing, in addition, a smectic A phase. The **4-N**12 and **4-N**13 homologues show only the smectic A phase between *ca.* 80 and 93 °C. In this series, a normal odd–even effect is clearly seen at the nematic-to-isotropic phase transition.

For the **3-N*n*** series, two comparisons can be made; first, with the structurally analogous cyano derivatives already described,[13] and secondly with the **4-N*n*** series to assess the relative merits of *meta* and *para* substitution. Comparison of the **3-N*n*** series with the analogous 3-cyanophenol–alkoxystilbazole (**3-C*n***) complexes revealed (Fig. 2) that the thermal stability of mesophases for the **3-N*n*** complexes was again typically 10–20 °C higher than that of their cyano counterparts. As with the **4-N*n*** series, the onset of the smectic behaviour was gradual, with intermediate derivatives being polymesomorphic. This is in contrast to the sudden change seen for the **3-C*n*** complexes, where **3-C**12 shows only a nematic phase and **3-C**13 only a smectic A phase.

Comparison of the phase behaviour of the **3-N*n*** series with that of the **4-N*n*** series shows the dramatic effect of structural isomerism. The fact that the **3-N*n*** complexes have a higher mesophase stability than their corresponding **4-N*n*** analogues indicates the importance of structural anisotropy. In the **3-N*n*** series, *meta* substitution counters the 'kink' induced in the structure by the hydrogen bond to the phenol. This explains the greater stability of the nematic phase (T_{NI} is at least 10 °C higher than in **4-N*n*** complexes) and the more pronounced odd–even effect (Fig. 2). The occurrence of the smectic A phase in both series is very similar appearing at about the same temperatures for given chain lengths.

Complexes of 2,4-dinitrophenol with 4-alkoxystilbazole (2,4-N*n*)

These complexes were bright yellow in contrast with all other series previously described, which were cream coloured. The phase behaviour is displayed in Fig. 4 and again, only nematic and smectic A phases were observed, although this time the phase diagram was of a different form. Thus, for short homologues (from **2,4-N**1 to **2,4-N**5), a monotropic nematic phase was seen at temperatures much lower than the melting points. Increasing the alkyl chain length saw a sudden transition to smectic behaviour, and from the **2,4-N**6 to the **2,4-N**13 derivative, a smectic A phase was observed. This was stabilised with increasing alkyl chain length, becoming enantiotropic from **2,4-N**8 and reaching a thermal stability of 126 °C in **2,4-N**13.

The mesomorphism of the **2,4-N*n*** complexes can be compared with both that shown by the **4-N*n*** and **3-N*n*** systems. Although the thermal stability of the nematic phase does not vary much within any given series, the stability is seen to increase in the order **2,4-N*n*** < **4-N*n*** < **3-N*n*** (Fig. 2). This parallels the increase in structural anisotropy, and is consistent with

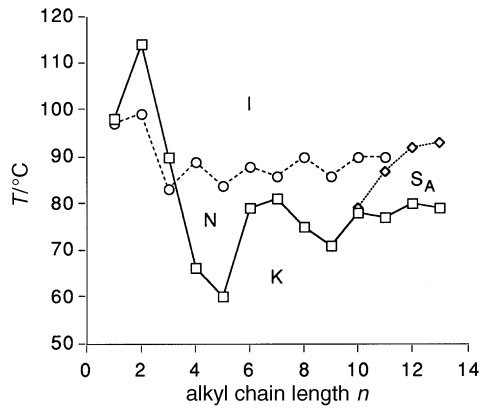

Fig. 3 The phase behaviour of the **3-N*n*** series: (□) K–, (◇) S_A–, (○) N–I

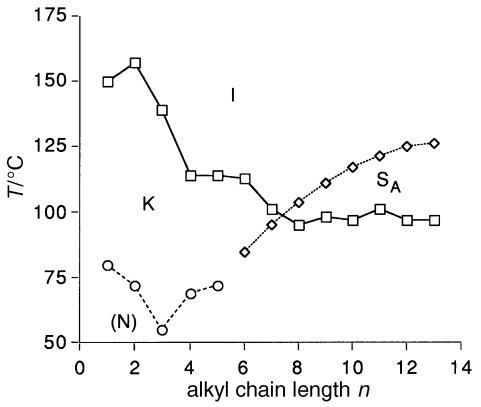

Fig. 4 The phase behaviour of the **2,4-N*n*** series: (□) K–, (◇) S_A–I, (○) N–I

Table 4 Small angle X-ray scattering data

complex	T/°C	t/T_{cl}	phase	d/Å	d_{calc}/Å[a]	d/d_{calc}
4-N12	85	0.93	S_A	45.7, 4.5	29.0	1.46
3-N12	85	0.92	S_A	43.0, 4.4	32.3	1.33
2,4-N12	105	0.84	S_A	47.2, 23.2, 4.4	31.3	1.5
3-N10	85	0.94	N	40.0, 4.5	29.0	1.37
2,4-N8	102	0.98	S_A	40.0, 19.3, 11.1, 4.4	26.0	1.54

[a]Molecular components calculated using CHEM 3D™ and hydrogen bonded distance from ref. 13.

the idea that formation of the nematic phase is related to the structural and polarisability anisotropies of the rigid core.

The stability of the smectic A phase as a function of chain length is shown in Fig. 5. In all series, the transition temperatures are seen to increase rapidly with increasing chain length beginning to 'level off' at longer homologues. The stability is clearly much greater in the **2,4-N*n*** series than in both **4-N*n*** and **3-N*n*** complexes, which are similar to one another. In addition, we note that smectic behaviour can be induced by a hexyloxy chain for the **2,4-N*n*** series, whereas nonyloxy or decyloxy chains are needed in the **4-N*n*** and **3-N*n*** series. That is, in these cases, much longer alkyl chains are required to produce the microphase separation of constituent parts that is the smectic A phase.

Despite the high acidity of 2,4-dinitrophenol ($pK_a = 3.96$),[15] the complex is still expected to exist predominantly in the non-ionic hydrogen bonded form,[16] on account of the small value of ΔpK_a [the difference between the pK_a of the conjugate acid of the stilbazole (*ca.* 5–6), and the pK_a of the phenol]. Although the complex is non-ionic (at least in the ground state[17]—*vide infra*), the increased acidity of the phenol strengthens the hydrogen bond, and increases its polarisability. Thus, the combination of increased polarisation due to having two nitro groups and increased polarisability (the hydrogen bond) that gives an additional stabilisation to the core–core interactions, disfavouring core–chain interactions, resulting in the predominance of the smectic A phase in the **2,4-N*n*** complexes.

X-Ray Scattering Studies

In our studies of the related 3-cyanophenol complexes,[13] we had in one case performed X-ray scattering experiments which clearly demonstrated that the S_A phase in question was interdigitated. X-Ray scattering studies were therefore carried out in the present case to obtain similar information. The data are collected in Table 4.

What the data clearly show is that the layer spacing in the S_A phase and the apparent molecular length in the nematic phase (**3-N**10 only) are significantly greater than the calculated molecular length. In the case of the S_A phase, this points to an interdigitated bilayer structure. However, the nematic cannot be interdigitated as it is not layered and so we must conclude here that we have the predicted antiparallel dimers as illustrated in Fig. 6. On this basis, we would assume that this arrangement existed in the S_A materials and was the cause of the increased layer spacing there, too.

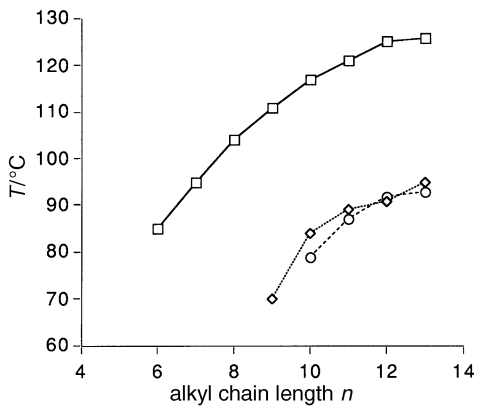

Fig. 5 The thermal stability of the smectic A phase (T_{S_AI} and T_{S_AN}) for complexes of (◇) **4-N*n***, (○) **3-N*n*** and (□) **2,4-N*n***

Thermodynamic Properties

From plots of entropy change as a function of chain length, n, for a particular transition in a given series, certain trends can be seen. In all cases crystal-to-isotropic liquid or crystal-to-mesophase transitions can be grouped together, as differences in entropy of the transition are typically much larger than the differences found between the isotropic liquid and mesophase. For all series we can see a general increase in ΔS with increasing homologue superimposed by a small parity dependence. However, as these values depend on factors, such as crystal structure, which have not been evaluated, then no meaningful comparison is possible here.

For the nematic-to-isotropic transition, enthalpies could only be obtained for the **4-N*n*** and **3-N*n*** series. Both series show no general trend with values in the range 1.0 to 3.4 J K^{-1} mol^{-1}. The **3-N*n*** series shows an odd–even effect, where even homologues show larger transition temperatures (T_{NI}) and larger entropies (ΔS_{NI}). That no great variation was observed is in agreement with the idea that increasing the alkyl chain length does nothing to stabilise or increase the order in the nematic phase, and that the origin of this phase derives primarily from the rigid core.

For the smectic A-to-isotropic transition, in all cases we see a clear increase in the entropy with increasing chain length. The data for the **4-N*n***, **3-N*n*** and **2,4-N*n*** series are shown graphically in Fig. 7. Unlike the nematic phase which has only one type of order—defined by the order parameter and related to the orientational distribution of molecules about the director—the smectic A phase has two. First, it has, like the nematic, a director and associated 'order parameter'. Secondly, there exists a one-dimensional periodicity giving it its layered structure. In liquid crystals, this positional ordering varies between two extremes. The most disordered case is a loose association that gives layers where the periodicity is best described by a sinusoidal distribution function. This is the case for many thermotropic liquid crystals, especially immediately below a nematic phase. At the other end, the lamellar structure can be very well defined, where the layers are much more 'rigid' and the periodicity approaches a series of Gaussian functions. This is typically the case found in lyotropic phases.

The similar structures of these complexes mean that comparison of their entropies is valid. So, first we make the assumption that the difference between entropies of the isotropic states, either within or between **2,4-N*n***, **4-N*n*** and **3-N*n*** complexes, is insignificant. This done, the changes in entropy of transition can be attributed to changes in the nature of the smectic A phases. Given that the entropies of the nematic-to-isotropic transition are more or less independent of alkyl chain length, no effect on the order parameter of the smectic A phase is expected for an increase in chain length. Thus, lower entropies correspond to a more sinusoidal distribution function, while

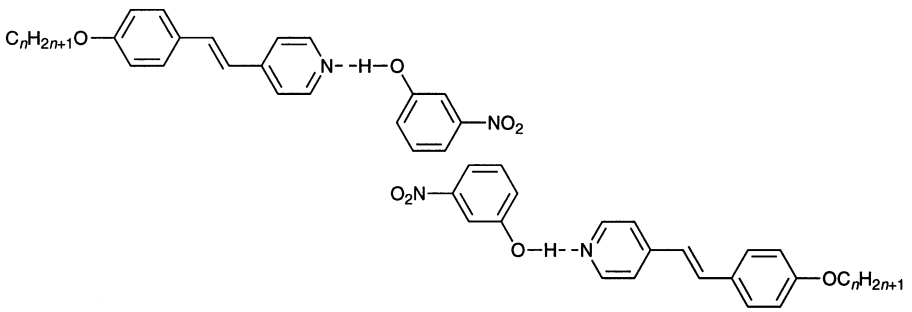

Fig. 6 The antiparallel structure adopted by the hydrogen bonded complexes

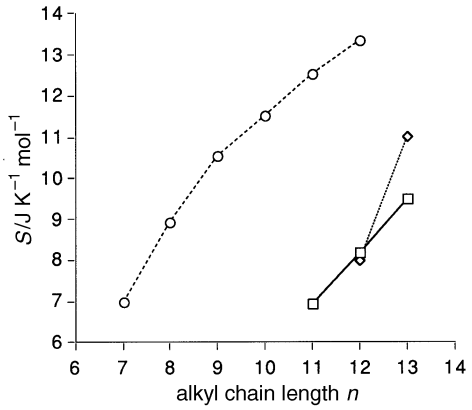

Fig. 7 The variation in entropy of the smectic A–isotropic transition for various homologues of the (□) **4-N*n***, (◇) **3-N*n*** and (○) **2,4-N*n*** series

higher values represent a greater deviation toward a Gaussian distribution.

Changes in the distribution function which describes the periodicity of the layers are solely a consequence of changes in the intermolecular interactions. By dividing molecules into two parts (the aromatic, polarisable core and the aliphatic chain), this system can be considered as containing only three types of pairwise interaction. These are core–core, chain–chain or core–chain interactions. In a rigidly layered system where cores are separated from chains, we have only core–core and chain–chain interactions. In a non-layered system, core–chain interactions would also be present.

When the energy of the core–chain interaction is too 'costly'—that is when the difference between interaction energies exceeds a certain threshold—the amount of core–chain interactions is reduced by forming a layered structure. Further increase in the 'cost' of this interaction causes a deviation from a purely sinusoidal distribution function towards a Gaussian one. These changes in distribution can be related to the entropy of the phase. Thus, through the nature of the distribution function, a larger value of ΔS can be related to a higher 'cost' of core–chain interactions. In this way we can see that changing the alkyl chain length, in a homologous series, can only effect chain–chain and core–chain interactions, and that the increase in ΔS with increasing homologue, n, reflects the stabilisation of chain–chain (or core–core) interactions above core–chain interactions. For the **2,4-N*n*** series we see that each additional carbon atom to the alkyl chain adds between 1 and 2 J K^{-1} mol^{-1} of order to the phase.

Comparison of the **2,4-N*n***, **4-N*n*** and **3-N*n*** series shows the structurally isomeric **4-N*n*** and **3-N*n*** complexes to have very similar behaviour, whereas the addition of an extra nitro group in the **2,4-N*n*** complex massively changes the order of the phase. The smectic A phase of the **2,4-N**12 derivative has an additional 5 J K^{-1} mol^{-1} (*ca.* 60%) of order than the **4-N**12 or **3-N**12 derivatives. It can also be said that smectic A-to-isotropic transitions with similar entropies will also have similar distribution functions. Thus, since **2,4-N**7 and **4-N**11 are almost isoentropic, they probably have similar phase structures. These conclusions are further supported by the X-ray data presented in Table 4 in which it is clearly seen that it is the two dinitrophenol complexes which show second and third order reflections for the lamellar spacings, again suggesting a more Gaussian distribution.

Binary Mixture Studies of 3-N8

Binary mixtures of various compositions were formed from 3-nitrophenol and 4-octyloxy-4′-stilbazole by a melt synthesis procedure. The phase behaviour of these mixtures was studied as a function of temperature using optical microscopy and DSC experiments. The results are shown in Fig. 8 as a binary phase diagram. The complexity of the phase behaviour is so great that even with the 15 compositions studied it is not possible to determine unambiguously the detailed structure of the phase diagram. The lines delimiting phase boundaries, eutectic and 'peritectic' like behaviour serve to highlight the gross behaviour, and are most likely the correct interpretation of the data.

The congruent melting behaviour observed at 50% 3-nitro-

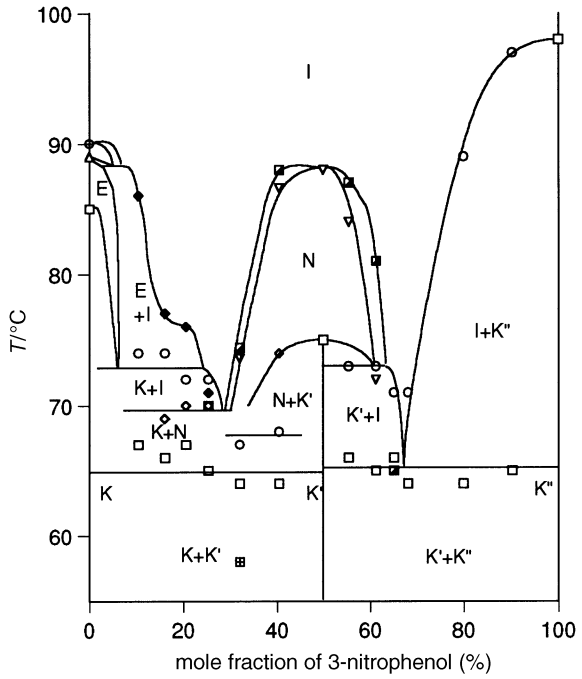

Fig. 8 The binary phase behaviour of mixtures of 3-nitrophenol and 4-octyloxy-4′-stilbazole: (□) K–, (◇) K + N–, (○) K + I–, (△) E–, (⊞) E + N–, (◆) E + I–, (⊕) S_B–, (▽) N–, (◪) N + I–

phenol (percentages are given as mole fractions of the two components) is conclusive evidence for the formation of a one-to-one adduct. This, and the increased thermal stability in the crystal and nematic phases at the 50% composition, implies complex formation is strongly favoured over the reverse reaction. It is consequently legitimate to treat the diagram as two separate halves: from 0 to 50% 3-nitrophenol, which in reality corresponds to a binary phase diagram of 4-octyloxy-4′-stilbazole with the complex **3-N**8; and from 50 to 100% 3-nitrophenol, which is the phase diagram of **3-N**8 with 3-nitrophenol.

For the right hand side of the diagram (50–100% 3-nitrophenol) the behaviour is that of two components whose isotropic liquid phases are completely miscible but do not form solid solutions. Here the eutectic point is formed at about 67% 3-nitrophenol with a melting point at *ca.* 65 °C. The nematic phase, is quickly destabilised becoming monotropic just above 60% 3-nitrophenol, and biphasic behaviour is seen at this clearing transition.

On the left hand side (0–50% 3-nitrophenol) the diagram shows the behaviour of mixtures of 4-octyloxy-4′-stilbazole and **3-N**8. This is much more complicated than the right hand side. It arises not only because now both of the components are mesomorphic, but also because different phases show differing degrees of miscibility. In particular while both crystal phases are immiscible, the smectic E phase shows a limited miscibility for a range of compositions. This is seen at the $E_{stilbazole} + I \rightarrow I$ transition, where a near flat phase boundary occurs at about 77 °C for compositions 85 to 80% stilbazole. This implies that the composition of the smectic E phase here is between 90 and 85% stilbazole, while the isotropic phase is relatively enriched in the complex **3-N**8.

It is not surprising that the crystal smectic E phase of the stilbazole is rather more tolerant of **3-N**8 impurity than the crystal phase. Given the more disordered nature of the smectic E phase, such behaviour is understandable. For these compositions the first transition on heating occurs at about 66 °C, and it is likely that the corresponding eutectic composition is at about 70% stilbazole. A final point worth noting is the overall stability of the nematic phase. The delimiting line, representing its uppermost thermal stability is unsymmetric across the whole phase diagram. The phase is tremendously destabilised by the non-mesogenic 3-nitrophenol, on the other hand, as one might expect, the mesogenic stilbazole impurity is quite well tolerated with relatively little depreciation in the phase stability.

Spectroscopic Investigations

Infrared studies

IR spectroscopy was used to examine the hydrogen bonding in these complexes. Samples were run as KBr discs and were examined between 4000 and 450 cm^{-1}. We acknowledge the suggestion[18] that KBr may not be an inert matrix for these hydrogen bonded adducts, as the possibility of a hydrogen bonded interaction with the bromide ion exists. However, identical spectra were obtained for a sample of solid **3-N**5 and this adduct in a KBr disc. We also note that the hydrogen bonded complexes of Yu and co-workers[8] prepared as Nujol mulls gave identical spectra to those in KBr discs. We believe that the changes in homologue and core structure of our complexes are unlikely to cause a change in the interaction with KBr.

The most obvious changes upon complexation are observed in the ν_{OH} region above 1700 cm^{-1}. The ν_{OH} band in the phenol at *ca.* 3200 cm^{-1} is replaced by a broad band in the complex centred at *ca.* 2500 cm^{-1} showing some substructure. This is indicative of the formation of a stronger hydrogen bond in the complex than in the pure phenol. Comparison of the spectral positions of the ν_{OH} stretching bands ranks the complexes in decreasing wavenumber such that **3-C**8 > **4-C**8 > **3-N**8 > **4-N**8. This suggests that the hydrogen bonding is strongest in the nitro derivatives, and that the 4-substitution gives a stronger hydrogen bond than 3-substitution. This is anticipated given the effect of these substituents upon the proton donating ability (which can be related to pK_a) of these phenols. The order is primarily attributed to the stronger electron-withdrawing properties of the nitro group over that of the cyano group, and secondarily the fact that any 3-substituted derivatives, unlike the 4-substituted, are not conjugated to the phenolic oxygen. The broad ν_{OH} band at *ca.* 2500 cm^{-1} suggests a 'weak' single minimum potential. This is anticipated for the monosubstituted adducts on the basis of the ΔpK_a values. However, with the increased acidity of the 2,4-dinitrophenol, an unsymmetric double minimum potential may be expected in the **2,4-N*n*** complexes.

When compared to **3-C*n***, **4-C*n***, the nitro-substituted adducts show additional bands. In the **3-N**8 and **4-N**8 complexes a broad band with a vibrational fine structure, centred at *ca.* 1800 cm^{-1}, is observed. This is more intense in the **4-N**8 derivative than the **3-N**8, and is not seen at all in the analogous cyano complexes. In **2,4-N**8 two additional bands at 2116 and 2022 cm^{-1} are seen. Although the hydrogen bond strength in **2,4-N**8 is expected to be comparable with carboxylic acid–pyridyl adducts, no similarity in the IR spectra is observed. Complexes of carboxylic acids and pyridyl moieties are described as forming intermediate to strong hydrogen bonds, and give rise to 'type i' spectra as defined by Hadzi,[19] showing a trio of bands, A–C at typically 2800, 2500 and 1800 cm^{-1}. The additional bands observed in **2,4-N**8 are probably overtones and combinations of other stretches.

Other noticeable changes are more subtle. Generally we see the pyridyl ν_{CN} stretch increase from 1590 cm^{-1} by *ca.* 10 cm^{-1} upon complexation. Similarly, the predominantly phenolic ν_{CO} increases by *ca.* 20 cm^{-1} to 1250 cm^{-1}. The magnitude and direction of each of these changes is as expected for the change in the environment for these groups.[20] The γ_{OH} and δ_{OH}, 'out-of' and 'in-plane' deformations of the pure phenols are not seen in the spectra of the adducts. These vibrations are believed to be responsible for the increase in background absorption[21] below 1300 cm^{-1}.

Variable temperature IR studies

Studies were performed on a sample of **3-N**5. The sample was heated under an argon atmosphere and spectra were recorded every 5 °C from room temperature (23 °C), to the isotropic phase at 140 °C. Other than a general loss of spectral resolution, two major changes were observed. The first was an unsymmetric broadening of the ν_{OH} band at *ca.* 2500 cm^{-1}, and a shift in position of the band maximum to higher frequencies. This shift and broadening of the ν_{OH} is consistent with a lengthening of the hydrogen bond, and an increased polarisability, reflecting the increased number of possible environments of this bond. Part of this region of the spectra is obscured by various ν_{CH} stretches, which are unaffected by the changes in temperature.

The second, and most impressive change was the complete and sudden loss of the band at *ca.* 1800 cm^{-1} upon melting. This broad, medium-intensity band, is present in the crystal at 60 °C, but disappears completely at 65 °C when the adduct has melted into the nematic phase. From this observation we can say that the band is in some way related to a lattice mode.

Solid state NMR studies

The timescale and sensitivity of the NMR experiment should reveal information about the average state of the hydrogen bonding, by changes in the chemical shifts of the atoms in the proximity of the interaction. Preliminary solid state MAS ^{13}C spectra were obtained for the complex **3-N**8 at ambient tem-

perature (23 °C) in the crystal phase, at 94 °C in the nematic state, and at 99 °C in the isotropic liquid. No discernible change was seen in these spectra, suggesting that in this complex the isotropisation is not driven by a dissociation of the complex into its constituent parts. Further, and more detailed studies are already underway.

Electronic spectroscopy of 2,4-N10

Unlike all of the other hydrogen bonded systems we have examined, the **2,4-N*n*** complexes are golden yellow. This is also in stark contrast to the components, the stilbazoles being cream coloured; λ_{max}(THF) 326 nm, and 2,4-dinitrophenol is a pale yellow; λ_{max}(THF) 295, sh 340 nm. The nature of the hydrogen bond greatly affects the electronic states in each conjugated chromophore. The large shift in the position of the absorption maxima experienced by both parts makes these complexes ideal for investigations by UV spectroscopy. Indeed the results of our preliminary studies have already been reported.[17]

The electronic spectra of **2,4-N**10—whose mesomorphism is Crys·97·S_A·117·I, was recorded every 0.33 °C at 90–126 °C. Reproducible spectra were obtained once the material had been allowed to crystallise. Fig. 9 shows a heating run from 90–118 °C; glass was used as a substrate giving a 'cut-off' point of *ca.* 310 nm. Fortunately, all major transitions are well above this value. In order to assign the spectra, it is useful to make comparison with certain fragments. In addition to the components (*vide supra*), we find that, decyloxystilbazolium chloride is bright yellow having a λ_{max}(THF) at 368 nm, and potassium 2,4-dinitrophenoxide is bright orange, λ_{max}(THF) 363 and 424 nm.

There are four bands in the spectra, A–D, and we have assigned each of these to the lowest energy transitions in 4-decyloxy-4′-stilbazole, 4-decyloxy-4′-stilbazolium, 2,4-dinitrophenol and 2,4-dinitrophenate, respectively. The observed isosbestic behaviour at 90–121 °C shows that only two species are present, which we identify as the non-ionic and ionic hydrogen bonded states (Scheme 1) and which shows that an increase in temperature populates the (excited) ionic state. Thus, the hydrogen bond clearly has an unsymmetric double minimum potential. That the non-ionic state is the ground state is also supported by the low value of the ΔpK_a between stilbazolium and 2,4-dinitrophenol, which is between 1 and 2. Lindemann and Zundel[16] suggest that usually a value of 4 is required to effect 50% proton transfer. Although comparisons of solution with solid state spectra, and predictions based on aqueous acidities, must be viewed with some caution, we feel

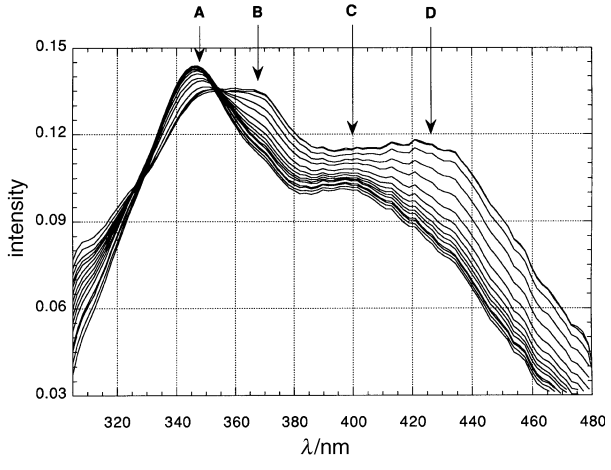

Fig. 9 Electronic spectra of the adduct **2,4-N**10 at 90–118 °C, as it passes from the crystal through the smectic A phase and into isotropic state

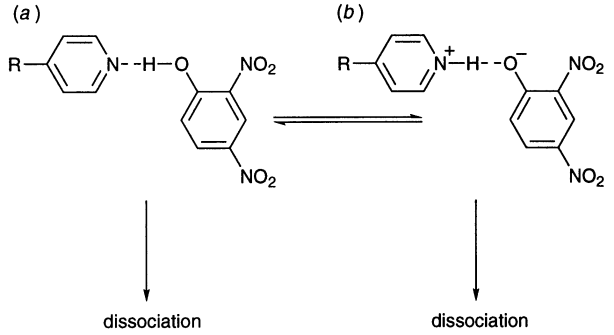

Scheme 1 Proton transfer between (*a*) the normal state of hydrogen bonding in the adduct and (*b*) the ionic hydrogen bonded form

that in the absence of more appropriate data such comparisons are acceptable.

The fact that isosbestic behaviour is observed up to 121 °C implies only one pair of species, and that no significant dissociation is seen up to this point. That is, isotropisation is driven by the structural anisotropy and properties of the complex as a whole, and not by the dissociation into constituent parts. It is informative to plot the intensities of the key transitions as a function of temperature and state; this is done in Fig. 10. Thus, bands B and D are seen initially to increase at the expense of band A. The transition C is apparently seen to increase, as it is not deconvoluted from bands B and D. Above 121 °C, we see the beginning of a general broadening of the spectra, a deviation from isosbestic behaviour, and a decrease in the intensities of all transitions. This is attributed to the dissociation of the complex from both ionic and non-ionic hydrogen bonded states. Dissociation from both of these states would lead to the observed hypsochromic and bathochromic shifts in the spectra. This would support the proposal from Kato[22] that dissociation does not occur until the isotropic state is reached and that, indeed, the fact that the hydrogen bonded complex is in a mesophase (particularly in the case of smectic phases) may serve to stabilise the hydrogen bond.

A final point to note concerns the relative populations of the two states. As both stilbazole and stilbazolium have similar extinction coefficients (30 600 and 33 000 $dm^3\,cm\,mol^{-1}$, respectively), we can say that a near 50% population is obtained above *ca.* 114 °C. However, a further increase in temperature above the clearing point sees a relative decrease in the population of the ionic hydrogen bonded state. To

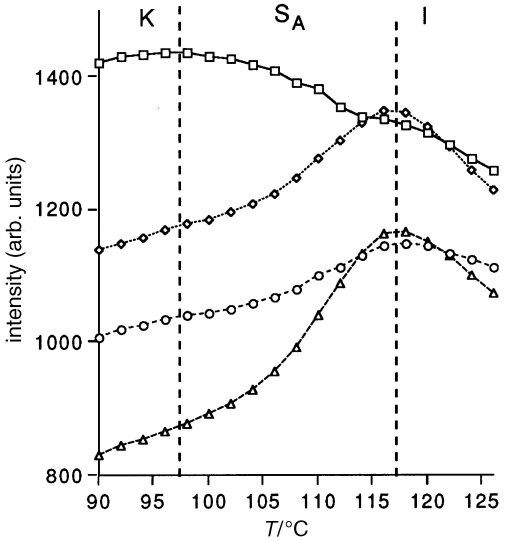

Fig. 10 The variation of the key transitions as a function of temperature: (□) 348 (A), (◇) 368 (B), (○) 400 (C) and (△) 426 nm (D)

account for this deviation from a normal thermal population of the ionic excited state, we propose that the environment of the smectic A phase, where there is a lamellar microphase separation of alkyl chains from the aryl cores, provides an additional stabilisation of the ionic hydrogen bonded state, as here the hydrogen bond is predominantly surrounded by polarisable (aryl groups) and polarised (nitro groups) functionalities. Thus, we re-emphasise the important conclusion that significant dissociation from the hydrogen bonded complexes does not occur until the isotropic state is reached and that isotropisation is not driven by a breakdown of the hydrogen bonded complex, indeed the mesophase may act to stabilise the hydrogen bond.

Experimental

Instrumentation

The components were characterised by microanalysis, performed at Sheffield University, and by ^{1}H and ^{13}C NMR on a Bruker WM250 spectrometer. Chemical shifts are quoted relative to an internal standard, and all coupling constants are given in Hz. ^{13}C NMR data were obtained from J-modulated spectra. All components gave satisfactory characterisation. Routine IR spectroscopy was performed, unless otherwise specified, as KBr discs on a Perkin Elmer 1600 series FTIR.

Variable temperature IR studies were performed using a Perkin Elmer 1710 FTIR equipped with an Infrared Associates Ltd NO 161373 liquid nitrogen cooled detector, working to a resolution of 4 cm^{-1}. The sample was deposited by evaporation from a diethyl ether solution onto a silicon rod, within a pressure cell. The cell was filled with argon to a pressure of 1 atmosphere at room temperature (23 °C) and sealed. The cell was then equipped with a heater and thermocouple and a temperature controlled to an accuracy of ± 5 °C. Attenuated total reflectance FTIR spectra were obtained every 5 K, through crystal, nematic and isotropic phases at 4000–200 cm^{-1}.

Tetrahydrofuran (THF) was refluxed under nitrogen over lumps of sodium and benzophenone until the solution became purple and was freshly distilled immediately prior to use.

Solution state electronic spectra were recorded on a Phillips PU8720 UV–VIS scanning spectrophotometer. The variable temperature 'solid' state electronic spectroscopy was performed in transmission, with a Photal Otsuka Electronics Deuterium Lamp, MC-962A and Spectromultichannel Photo Detector, MCPD-100. The sample was heated on a Mettler hot stage with an FP90 control processor. Heating rates of 1 and 4 K min^{-1} were employed and spectra were taken every 0.33 or 1 K. Samples were prepared by placing a saturated solution of the material in tetrahydrofuran onto a glass microscope slide, covering with a coverslip and allowing the solvent to evaporate at *ca.* 60 °C.

The mesomorphism was characterised by heated stage polarising optical microscopy, using a Zeiss Labpol microscope fitted with a Linkam TH600 hot stage and a PR600 temperature controller. Enthalpies of transitions were recorded by a Perkin Elmer DSC 7 instrument, at heating and cooling rates of between 5 and 10 K min^{-1} were employed.

X-Ray diffraction patterns were recorded with an Image Plate area detector (MAR Research) using graphite-monochromatised Cu-Kα pinhole collimated radiation. The samples, in glass capillaries, were held in a temperature-controlled cell. The beam path was flushed with helium.

Components

3-Nitrophenol (BDH) was crystallised from water. 2,4-Dinitrophenol (BDH) was dried under high vacuum and 4-nitrophenol (Hopkin and Williams Ltd) was used without further purification. 4-Alkoxy-4′-stilbazoles were synthesised in good yield by coupling 4-methylpyridine and the corresponding 4-alkoxybenzaldehyde, followed by an acid-catalysed elimination to convert the intermediate secondary alcohol into the product. The procedure is described for the butoxy derivative. Analogous procedures were employed for all other homologues. All components gave satisfactory characterisation. The behaviour of the stilbazoles was identical to that of authentic samples.[14]

General sample preparation

Complexes were formed by dissolving exactly equimolar amounts of the components in tetrahydrofuran and removing the solvent on a rotary evaporator. The compromise to purity that mixing brings is estimated to be not more than 1%.

Mixture preparation

Homogeneous mixtures were formed from solutions of the components, by removing the solvent (tetrahydrofuran) at *ca.* 60 °C, then heating the mixture while stirring with a magnetic follower, at up to *ca.* 120 °C, where only a single isotropic phase is present, and then cooling quickly.

1-(4-Butoxyphenyl)-2-(4-pyridyl)ethanol. A solution of diisopropylamine (3.757 g, 37.2 mmol), in dry tetrahydrofuran (200 cm^3; freshly distilled from sodium benzophenone ketyl), was cooled under a nitrogen atmosphere to −78 °C. Butyllithium (23.5 cm^3, 1.6 mol dm^{-3} solution in hexanes, 37.6 mmol) was added dropwise over a period of 40 min. The reaction was allowed to stir for a further 30 min while a temperature of −78 °C was maintained. After this time a solution of 4-methylpyridine (3.459 g, 37.2 mmol) in tetrahydrofuran (30 cm^3) was added dropwise over 1 h. The reaction mixture, which became bright orange, indicating the formation of the carbanion, was stirred for a further 40 min. Subsequent dropwise addition of 4-butoxybenzaldehyde (6.0 g, 33.7 mmol) in tetrahydrofuran (30 cm^3) over 30 min was accompanied by a colour change of the reaction mixture from orange to pale yellow. The mixture was stirred for 30 min and then allowed to warm to room temp. over 3 h. The excess pyridyl carbanion was quenched with water (20 cm^3), upon which the reaction became instantly colourless, the mixture was then neutralised with dilute aqueous hydrochloric acid. All of the solvents were removed under reduced pressure on a rotary evaporator. The solid was partitioned between dichloromethane (200 cm^3) and water (3×200 cm^3) and washed once with saturated brine solution (1×200 cm^3). The organic phase was dried over anhydrous magnesium sulfate, filtered and the solvent removed on a rotary evaporator, giving the crude product as an oil which crystallised upon standing. Recrystallisation from heptane gave the product (yield 4.95 g, 18.3 mmol, 54%). mp 87 °C (found: C, 75.1; H, 7.8; N, 5.2. $C_{17}H_{21}NO_2$ requires: C, 75.3; H, 7.8; N, 5.2%); ν_{max} cm^{-1} (KBr) ν_{O-H} 3202 br vs; δ_H (250 MHz; $CDCl_3$) 0.97 (3H, H_a, t, $^3J_{ac}$ 9.4), 1.40–1.58 (2H, H_b, m), 1.68–1.82 (2H, H_c, m), 2.93 (1H, H_j, dd, *J* 16.9, 6.9), 3.03 (1H, H_j, dd, *J* 16.9, 10.0), *ca.* 3.0 (1H, H_n, br s), 3.94 (2H, H_d, t, $^3J_{cd}$ 8.1), 4.85 (1H, H_i, dd, *J* 10.0, 6.9), 6.84 (2H, H_f, AA′XX′, *J* 10.6), 7.05 (2H, H_l, AA′XX′, *J* 7.5), 7.20 (2H, H_g, AA′XX′, *J* 10.6) and 8.35 (2H, H_m, AA′XX′, *J* 7.5); δ_C (63 MHz; $CDCl_3$) 13.9 C_a, 19.6 C_b, 31.3 C_c, 45.1 C_j, 67.7 C_d, 74.0 C_i, 114.4 C_f, 125.0 C_l, 127.1 C_g, 135.6 C_h, 147.8 C_k, 149.3 C_m and 158.8 C_e.

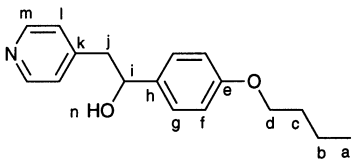

trans-4-*Butoxy*-4′-*stilbazole* {*trans*-4-[2-(4-butoxyphenyl) ethenyl]pyridine}. To a solution of 1-(4-butoxyphenyl)-2-(4-pyridyl)ethanol (4.921 g, 18.15 mmol) in toluene (300 cm^3) was added toluene-*p*-sulfonic acid (10.021 g, 56.26 mmol) and pyridine (4.430 g, 56.08 mmol). The reaction mixture was heated under reflux overnight and a Dean–Stark apparatus was used to remove the water produced by azeotropic distillation. After cooling, a solution of potassium hydroxide (3.614 g, 64.42 mmol) in a mixture of water (200 cm^3) and ethanol (5 cm^3) was added, and the reaction stirred for a further 12 h. The phases were separated and the organic layer washed with water (5×200 cm^3) and saturated brine (1×200 cm^3). The toluene solution was then dried over anhydrous magnesium sulfate, filtered and the solvent removed under reduced pressure. Crystallisation from hot acetone gave the product, *trans*-4-butoxy-4′-stilbazole (yield 3.371 g, 11.21 mmol, 62%). mp 95 °C (lit.,[14] 95 °C) (found: C, 80.34; H, 7.56; N, 5.57. $C_{21}H_{19}ON$ requires: C, 80.60; H, 7.56; N, 5.53%); δ_H (250 MHz; $CDCl_3$) 0.97 (3H, H_a, t, $^3J_{ab}$ 7.5), 1.49 (2H, H_b, m), 1.77 (2H, H_c, m), 3.98 (2H, H_d, t, $^3J_{dc}$ 6.4), 6.77 (1H, H_j, d, $^3J_{ij}$ 16.2), 6.83 (2H, H_g, AA′XX′, *J* 8.4), 7.15 (1H, H_i, d, $^3J_{ij}$ 16.2), 7.22 (2H, H_l, AA′XX′, *J* 6.1), 7.38 (2H, H_f, AA′XX′, *J* 8.4) and 8.46 (2H, H_m, AA′XX′, *J* 6.1); δ_C (63 MHz; $CDCl_3$) 13.9 C_a, 19.2 C_b, 31.3 C_c, 67.8 C_d, 114.8 C_f, 120.6 C_l, 123.6 C_j, 128.4 C_g, 128.7 C_h, 132.8 C_i, 145.0 C_k, 150.1 C_m and 159.8 C_e.

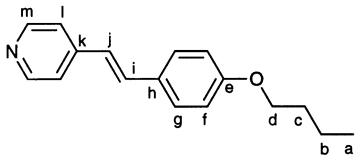

We would like to thank the EPSRC for a studentship to D. J. P., Dr David Apperly (EPSRC Solid State NMR service, Durham) for his invaluable assistance with solid state MAS NMR and Dr Tony Haynes (Sheffield) for his assistance with variable-temperature infrared studies. We wish to thank Professor Günter Lattermann (Bayreuth) for suggesting the potential benefits of a nitro group in these systems.

References

1 D. Vorländer, *Z. Phys. Chem.*, 1923, **105**, 211; G. M. Bennett and B. Jones, *J. Chem. Soc.*, 1939, 420.
2 C. Eaborn, *J. Chem. Soc.*, 1952, 2840; A. Polishchuk, T. V. Timofeeva, N. N. Makarova, M. Yu. Antipin and Yu. T. Struchov, *Liq. Cryst.*, 1991, **9**, 433.
3 J. D. Bunning, J. E. Lydon, C. Eaborn, P. M. Jackson, J. W. Goodby and G. W. Gray, *J. Chem. Soc., Faraday Trans. 1*, 1982, 713.
4 F. Henrich, S. Diele and C. Tschierske, *Liq. Cryst.*, 1994, **17**, 827.
5 For reviews of this subject see: G. A. Jeffery and L. M. Wingert, *Liq. Cryst.*, 1992, **12**, 179; G. A. Jeffery, *Acc. Chem. Res.*, 1986, **19**, 168.
6 C. Paleos and D. Tsiourvas, *Angew. Chem., Int. Ed. Engl.*, 1995, **34**, 1696.
7 M. Kotera, J.-M. Lehn and J.-P. Vigneron, *J. Chem. Soc., Chem. Commun.*, 1994, 197; M.-J. Brienne, J. Gabard, J.-M. Lehn and I. Stibor, *J. Chem. Soc., Chem. Commun.*, 1993, 420.
8 L. J. Yu, J. M. Wu and S. L. Wu, *Mol. Cryst. Liq. Cryst.*, 1991, **198**, 407; L. J. Yu and J. L. Pan, *Liq. Cryst.*, 1993, **14**, 829; L. J. Yu, *Liq. Cryst.*, 1993, **14**, 1303.
9 C. M. Lee, C. P. Jarwala and A. C. Griffin, *Polymer*, 1994, **35**, 4550.
10 D. J. Price, PhD thesis, Sheffield University, 1995; H. Kihara, T. Kato, T. Uryu, S. Ujiie, K. Iimura, U. Kumar, J. M. J. Fréchet, D. W. Bruce and D. J. Price, *Liq. Cryst.*, 1996, **21**, 25; D. J. Price, H. Adams and D. W. Bruce, *Mol. Cryst. Liq. Cryst.*, 1996, **289**, 127; K. Willis, J. E. Luckhurst, D. J. Price, J. M. J. Fréchet, H. Kihara, T. Kato, G. Ungar and D. W. Bruce, *Liq. Cryst.*, 1996, **21**, 585.
11 T. Kato and J. M. J. Fréchet, *J. Am. Chem. Soc.*, 1989, **111**, 8533; T. Kato and J. M. J. Fréchet, *Macromolecules*, 1989, **22**, 3818; U. Kumar, T. Kato and J. M. J. Fréchet, *J. Am. Chem. Soc.*, 1992, **114**, 6630; T. Kato, H. Kihara, T. Uryu, A. Fuijishima and J. M. J. Fréchet, *Macromolecules*, 1992, **25**, 6836; T. Kato, H. Kihara, U. Kumar, T. Uryu and J. M. J. Fréchet, *Angew. Chem., Int. Ed. Engl.*, 1994, **33**, 1644; T. Kato, P. G. Wilson, A. Fuijishima and J. M. J. Fréchet, *Chem. Lett.*, 1990, 2003; T. Kato, J. M. J. Fréchet, P. G. Wilson, T. Saito, T. Uryu, A. Fuijishima, C. Sin and F. Kaneuch, *Chem. Mater.*, 1993, **5**, 1094; T. Kato, A. Fuijishima and J. M. J. Fréchet, *Chem. Lett.*, 1990, 912; M. Fukumassa, T. Kato, T. Uryu and J. M. J. Fréchet, *Chem. Lett.*, 1993, 65; T. Kato, H. Kihara, T. Uryu, S. Ujiie, K. Iimura, J. M. J. Fréchet and U. Kumar, *Ferroelectrics*, 1994, **148**, 1303.
12 D. W. Bruce and D. J. Price, *Adv. Mater. Opt. Electron.*, 1994, **4**, 273.
13 H. Adams, D. W. Bruce, D. J. Price, G. Ungar and K. Willis, *J. Mater. Chem.*, 1995, **5**, 2195.
14 D. W. Bruce, D. A. Dunmur, E. Lalinde, P. M. Maitlis and P. Styring, *Liq. Cryst.*, 1988, **3**, 385.
15 *CRC Handbook of Chemistry and Physics*, ed. D. R. Lide, 75th edn., CRC Press Inc., Boca Raton, Florida.
16 R. Lindemann and G. Zundel, *J. Chem. Soc., Faraday Trans. 2*, 1972, **68**, 979; R. Lindemann and G. Zundel, *J. Chem. Soc., Faraday Trans. 2*, 1977, **73**, 788.
17 D. J. Price, T. Richardson and D. W. Bruce, *J. Chem. Soc., Chem. Commun.*, 1995, 1911.
18 K. R. Seddon, personal communication, 1995.
19 D. Hadzi, *Pure Appl. Chem.*, 1965, **11**, 435.
20 D. W. Brown, A. J. Floyd and M. Sainsbury, *Organic Spectroscopy*, Wiley, Bath, 1988.
21 S. L. Johnson and K. A. Rumon, *J. Phys. Chem.*, 1965, **69**, 74.
22 T. Kato, personal communication.

Paper 7/00575J; *Received* 24*th January*, 1997